AIAA SciTech Forum
7-11 January 2019, San Diego, California
AIAA Scitech 2019 Forum

10.2514/6.2019-1968

Determining the Master Curve of Aged Solid Propellant Using a Dynamic Mechanical Analyzer

Charles S. Wojnar*
Missouri University of Science and Technology, Rolla, Missouri, 65409, USA.

Timothy C. Miller† and Kamran B. Ghiassi‡
Air Force Research Laboratory, Edwards Air Force Base, California, 93524, USA.

Understanding aging in solid propellants is important for predicting the service lifetime of solid rocket motors in aerospace and defense applications. The accurate measurement of the master curve of the propellant is necessary for input into finite element simulations of fracture and debonding in solid rocket motors that lead to their failure. The use of a dynamic mechanical analyzer over conventional stress relaxation tests presents several advantages including smaller specimen size, which simplifies the artificial aging procedure, and results in improved accuracy due to the application of smaller strains. A method is presented for measuring the master curve of a particular propellant, viz. hydroxyl-terminated polybutadiene (HTPB), using a dynamic mechanical analysis setup. Specimens were artificially aged at 50 and 60 °C for durations ranging from one to eight weeks in order to approximate up to six years of natural aging at room temperature. The measured master curves show that increasing the artificial aging time at 60 °C leads to a higher relaxation modulus for a given reduced time. This is attributed to higher cross-link density in aged HTPB specimens. Aging at 50 °C for the given durations shows less of an effect, which indicates that 50 °C is not a sufficiently high temperature for inducing aging in the time periods studied for the manufactured specimens. The measured master curves can be used to inform material models such as Prony series in finite element simulations for predicting the lifetime of solid rocket motors.

I. Introduction

Hydroxyl-terminated polybutadiene (HTPB) is a widely used propellant binder in solid rocket motors. The ability to accurately predict the lifetime of such solid rocket motors will reduce the required number of destructive tests of motors as well as the likelihood of failure [1–3]. The stress relaxation over time of solid propellant is an important factor for predicting lifetime. Indeed, Prony series representations of stress relaxation curves are often utilized in finite element simulations of solid rocket motors to predict thermal stresses, debonding, and failure over extended periods of time [4, 5]. Due to their potential storage under wide ranges of temperatures and lengths of time, the stress relaxation response of solid propellant must be measured for various combinations of elapsed time and temperature, which is captured in the material's master curve. The master curve is obtained by appropriate time-temperature superposition, which is commonly accomplished via the Williams-Landel-Ferry (WLF) [6] equation. The master curve can then be used to generate a temperature-dependent Prony series to be implemented in finite element simulations. These approaches follow viscoelasticity theory and assume a thermorheologically-simple response [7]. However, aging affects the solid propellant's viscoelastic response. Thus, it is important to understand how aging affects the master curve of solid propellant in order to incorporate such effects into models for predicting the service life of motors.

Aging in solid propellant is important due to the storage time of solid rocket motors (as long as decades) before usage. Aging occurs in solid propellant through various mechanisms including cross-linking of HTPB and dewetting. For HTPB-based propellant, cross-linking is typically the dominant aging mechanism [8] due to the formation of side-chain branches during polymerization. These side-chains are a source of cross-linking, causing the propellant to have a higher elastic modulus and fail in a brittle fashion. This may lead to fracturing and debonding of the propellant grain after storage for extended periods of time [9]. The new surface area created by fractures and debonded regions alters the propellant's burning rate and can lead to failure of the solid rocket motor [10]. Failure models require the

---

*Assistant Professor, Mechanical and Aerospace Engineering, 400 W. 13th St., Rolla, MO 65409.

†Materials Research Engineer, Propellants Branch, Air Force Research Laboratory, Edwards Air Force Base, CA 93524.

‡Research Chemist, Air Force Research Laboratory, Edwards Air Force Base, CA 93524.

Copyright © 2019 by the American Institute of Aeronautics and Astronautics, Inc. All rights reserved.

stress and strain distribution in the motor to be known. Hence, obtaining the viscoelastic response, through the master curve, will enable the accurate prediction of stress and strain in solid rocket motors under various loading conditions.

Current approaches for determining the master curve of aged propellant involve the artificial aging of specimens followed by a series of stress-relaxation tests at different temperatures using a uniaxial loading frame. The natural aging process in solid rocket motors takes place over many years due to the aforementioned time-dependent processes such as cross-linking and dewetting. To observe these aging affects in a reasonable laboratory time scale, specimens must be artificially aged at elevated temperatures in ovens to accelerate the kinetics of the aging mechanisms. Due to the combustible nature of the material, the ovens must be explosion resistant. Generally, the safety requirements become greater as the specimen sizes become larger. Thus, smaller specimen sizes are preferred for simplifying the complexity and cost of the artificial aging process. A second drawback of current tensile testing methods is that many mechanical testing laboratories utilize large tensile loading frames, which require the application of large stresses and strains to have sufficient resolution. However, these large stresses and strains can lead to nonlinearity of the response and damage (e.g. due to dewetting). This complicates the prediction of the material's linear viscoelastic response. Moreover, the induced damage requires new specimens to be used for each test. Generating the master curve for the material requires many stress relaxation tests at different temperatures, hence a significant number of specimens is required, which increases the amount of material and time required. Thus, an approach that only applies small stresses and strains would save time and material. For these two reasons, a dynamic mechanical analyzer is desirable due to the smaller required specimen size and its high accuracy stress and strain measurement, which ensures linear viscoelastic conditions. Here, we present a method for artificially aging propellant specimens and measuring their master curve using a dynamic mechanical analyzer. In particular, master curves are obtained for differently-aged HTPB-based propellant. This approach reduces the material and time required for characterizing the effect of aging on the master curve of solid rocket propellants.

While the approach presented here using a dynamic mechanical analyzer to generate master curves is used instead of traditional tension tests, this approach does not completely replace tension tests. For characterizing the failure of propellant, for example, one must still carry out pull-to-failure tests. However, the main focus here is on obtaining the master curve of the relaxation modulus in order to better predict the behavior of propellant under storage conditions.

II. Experimental Methods

The following sections provide details on the method used to prepare the aged specimens. Then the experimental apparatus and procedure is described. Finally, the data analysis procedure is discussed.

A. Specimen Preparation

The HTPB-based propellant used in experiments contained the following ingredients with solids loading between 85-90 %. Please note that due to the restricted nature of the propellant formula, only a range is provided for the ingredients: ammonium perchlorate as the oxidizer (AP, bimodal particle size distribution, 65-70 %), aluminum as a fuel (17-20 %), iron oxide as a burn rate modifier (0.25-1 %), triphenylbismuth (TPB, 0.001-0.01 %) as a catalyst, isophorone diisocyanate (IPDI, 0.25-1 %) as a curative, dioctyl adipate (DOA, 1-5 %) as a plasticizer, and an antioxidant (AO 2246, 0.1-1 %). Specimens were cut from a single casted block of propellant (i.e. they came from the same mix); 3.5 mm thick slabs were milled from the block and then hand cut using a razor to the nominal dimensions of $60 \times 12.5 \times 3.5$ mm^3. Specimens weighed approximately 5 g.

To achieve realistic levels of aging in a laboratory time scale, specimens were artificially aged at elevated temperatures for extended periods of time to mimic aging at room temperature (assuming a thermorheologically-simple response.) Different levels of aging were achieved by placing specimens in ovens at either 50 or 60 °C. The relative humidity was maintained below 50 %. At each temperature, specimens were stored in the oven for durations of 1, 2, 4, and 8 weeks. Explosion-resistant Tenney temperature chambers were used to age the specimens, which were stored in velostat bags (loosely wrapped) inside the chambers for the required durations. There are various methods for storing specimens in the temperature chambers (e.g. in glass stoppers or in aluminum foil [11]), but velostat is one of the most common methods. It should be noted that the way the specimen is stored in the oven can significantly affect the aging process. Different material used to cover the specimen can vary the amount of oxidation that occurs [11]. The velostat bags are not impermeable to oxygen and care must be taken when using the measured data to compare with solid rocket motors that may have different levels of antioxidant protection. Besides oxidation, diffusion of plasticizer is also affected by the choice of material used to store the specimens. Quantifying the equivalent aging of specimens via exposure to elevated temperatures is an open challenge. The multiple aging mechanisms (e.g. the diffusion of different species and different types of cross-linking), their relative kinetics, and variation in composition and manufacturing processes

Table 1 Specimen aging procedures and resulting WLF parameters

Specimen	Aging Temperature (°C)	Aging Time (weeks)	Natural Aging Time (years)	c_1 (log(min.))	c_2 (°C)
A	50	1	0.3	10.44555	179.4356
B	50	2	0.6	20.06591	308.8927
C	50	4	1.2	12.16564	182.5339
D	50	8	2.4	10.65594	147.8412
E	60	1	0.75	17.33936	269.8837
F	60	2	1.5	10.01911	162.2722
G	60	4	3	12.16563	182.5338
H	60	6	6	33.94792	459.3066
I		Unaged		11.25821	188.3922

complicates the prediction of equivalent aging time. Nonetheless, empirical relations between artificial aging times and their corresponding equivalent age have been determined. Of course, such relations are highly dependent on the specific composition, manufacturing process, and environmental conditions. However, to obtain an estimate of the equivalent aging time, we adopt the empirical relation in [12, 13], which was obtained for a specimen of HTPB propellant,

$$t_E = \frac{t_T}{365.25} F^{(T_T - T_E)/\Delta T_F}, \tag{1}$$

where t_E is the equivalent natural aging time in years at a temperature T_E for a given heat treatment at T_T for a number of days t_T. The change in reaction rate factor for a change in temperature ΔT_F is given by the parameter F. We assume the same values previously used for a type of HTPB-based propellant, where $F = 2.5$ and $\Delta T_F = 10$ °C [12, 14]. Again, we caution that the parameter values used here depend on the aging mechanisms present, which result from the specimen composition, processing, and environmental conditions. We simply use them here to estimate the equivalent age. Using this relation, the corresponding estimated natural aging times for the specimens are given in Table 1, where the natural aging temperature was taken to be at 20 °C. The last two columns show the parameters associated with the WLF equation (2) obtained from experiments (as discussed in the next section.)

After artificial aging, specimens were wrapped in velostat bags and stored in an air-conditioned facility at room temperature for five months until they were tested. The relative humidity was maintained below 50 %. During this five month period, the Shore A hardness of the specimens were measured at regular intervals until it reached a steady state, which ensured that any curing effects had subsided (see Fig. 1). Besides the aged specimens, an unaged specimen was produced by storing a specimen at room temperature in a velostat bag for the same time duration. Immediately prior to mechanical testing, specimens were taken out of their velostat bag and placed in the testing machine, exposing the specimen to room conditions for approximately five minutes.

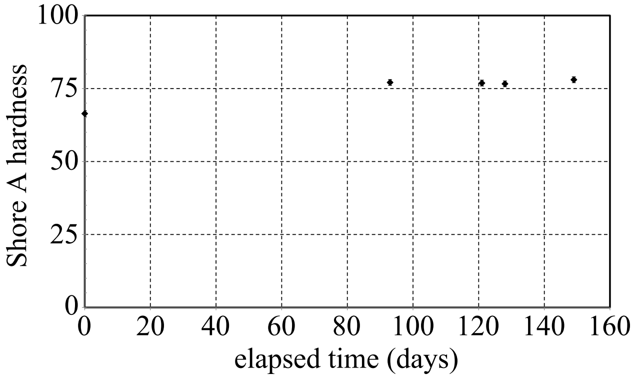

Fig. 1 Shore A hardness of a specimen after manufacturing.

B. Experimental Setup

Stress relaxation experiments were carried out using a commercial Dynamic Mechanical Analyzer (DMA) (TA Instruments Q800) as shown in Fig. 2(a). Specimens were tested using the double cantilever beam (DCB) fixture as shown in Fig. 2(b). As discussed in previous sections, the DMA was used instead of traditional uniaxial tension tests due to its higher accuracy and smaller required specimen size. In addition, DMA testing ensured that linear viscoelastic constitutive theories were valid due to its capability of applying sufficiently-small strains. In the Q800 DCB fixture, the deformable specimen length was 35 mm. Specimens were equilibrated at the desired temperature for 30 minutes and then a constant displacement was applied to the center of the cantilever beam. The strain is not uniform in the sample since it is subjected to bending. A nominal displacement of 95 μm was applied and was chosen such that the maximum strain in the specimen was 0.25 %, which was determined to be in the material's linear viscoelastic regime in a previous study [15]. For brevity in the following, a specified applied strain refers to the maximum strain (i.e. on the tensile side of the specimen.) The resulting applied force was measured and was used by the instrument's software to determine the material's relaxation modulus versus time; the Q800 uses beam theory solutions as well as corrections to account for shearing in thick specimens when determining the relaxation modulus. This value of the relaxation modulus was also verified to be consistent with the measured value from uniaxial tension tests [15].

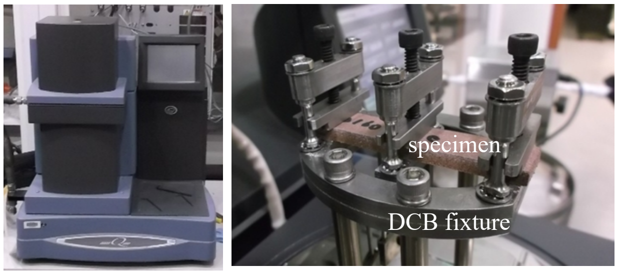

a) b)

Fig. 2 Experimental setup showing (a) the TA Q800 dynamic mechanical analyzer with (b) a test specimen placed in the double cantilever beam fixture.

The procedure for carrying out the stress relaxation test begins by first placing the specimen in the DCB fixture with the grips initially loose. The environmental chamber was closed and the specimen was equilibrated to the desired temperature over 5 minutes; experiments at various temperatures are required to obtain the master curve as described in later sections. After 5 minutes, the temperature had reached steady state and the specimen contracted or expanded (due to the temperature change.) Leaving the grips loose during temperature equilibration eliminates thermal stress, which was observed to significantly affect the results in a previous study [15]. Then the environmental chamber was immediately opened and the fixture grips tightened to approximately 0.2 N·m. It is important not to over tighten the clamps as this will cause large deformations in the specimen around the clamps and render the computed relaxation modulus inaccurate. The environmental chamber was then closed again and the procedure continued by equilibrating again for 5 minutes to the desired temperature (a prestrain of 0.01 % corresponding to a 3.8 μm displacement was simultaneously applied to eliminate slack.) After reaching steady state, the temperature was then held fixed for another 30 minutes to ensure thermal equilibrium (while still applying a prestrain of 0.01 % to remove slack.) This is referred to as the "isothermal" portion of the test, which corresponds to the function in the DMA's software.

After starting the data acquisition, the strain was then ramped to the desired level (0.25 %) at a rate of 12 %/minute, which was the fastest rate possible by the DMA. Then, the strain was held fixed at 0.25 % at the selected temperature for 30 minutes using the "isothermal" function. This ramp and hold portion of the experiment constitutes the stress relaxation test. After the relaxation test, the strain was ramped back to 0.01 % at a rate of 12 %/minute. This process (including loosening and re-tightening of the clamps) was repeated at each level of temperature. The levels of temperature used to generate the master curve (in order of testing) were -30, -15, 0, 20, 40, and 60 °C. A flow chart of the aforementioned steps is shown in Fig. 3.

C. Generating the Master Curve

The master curve was generated from the stress relaxation curves measured at each temperature. Only the data after ten times the rise time in the stress relaxation response was used to generate the master curve. The rise time was taken as the time for the applied strain to first reach the prescribed level from the initial prestrain level. Neglecting this data

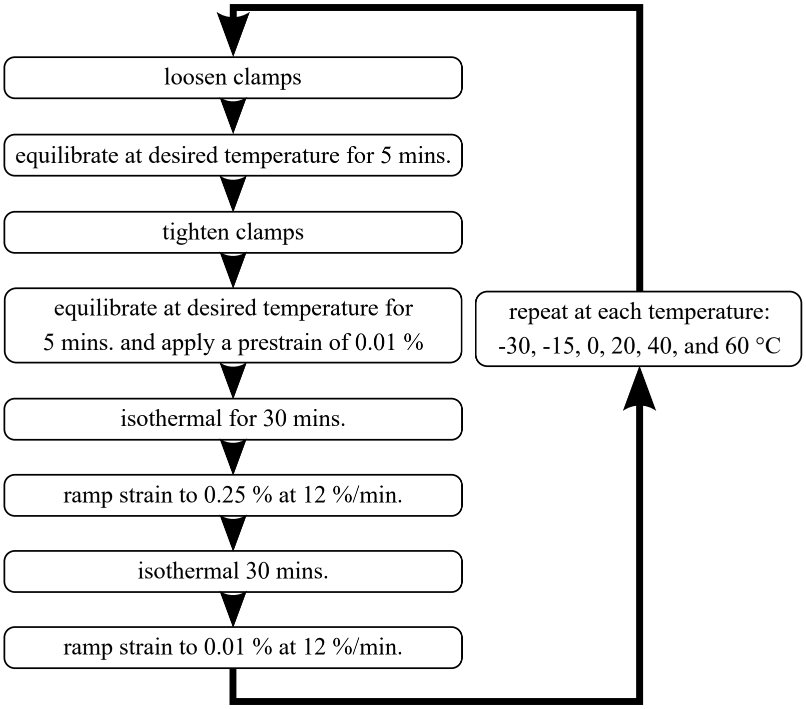
loosen clamps
equilibrate at desired temperature for 5 mins.
tighten clamps
equilibrate at desired temperature for 5 mins. and apply a prestrain of 0.01 %
isothermal for 30 mins.
ramp strain to 0.25 % at 12 %/min.
isothermal 30 mins.
ramp strain to 0.01 % at 12 %/min.
repeat at each temperature: -30, -15, 0, 20, 40, and 60 °C

Fig. 3 Flowchart showing the procedure used to measure the master curve.

removes the effect of variations in the strain ramp profile. The stress relaxation curve is shifted on a logarithmic axis by dividing the time by a shift parameter, a_T, such that a continuous stress relaxation curve between each temperature is obtained. The shift parameter as a function of temperature T is assumed to be given by the WLF equation [6],

$$\log a_T = -\frac{c_1(T - T_{\text{ref}})}{c_2 + (T - T_{\text{ref}})}, \tag{2}$$

where the reference temperature was taken to be $T_{\text{ref}} = 20$ °C. The parameters c_1 and c_2 were obtained for each specimen via a least squares fit to the experimental data and are shown in Table 1. An example curve fit of the WLF equation obtained for the unaged specimen, I, is shown in Fig. 4.

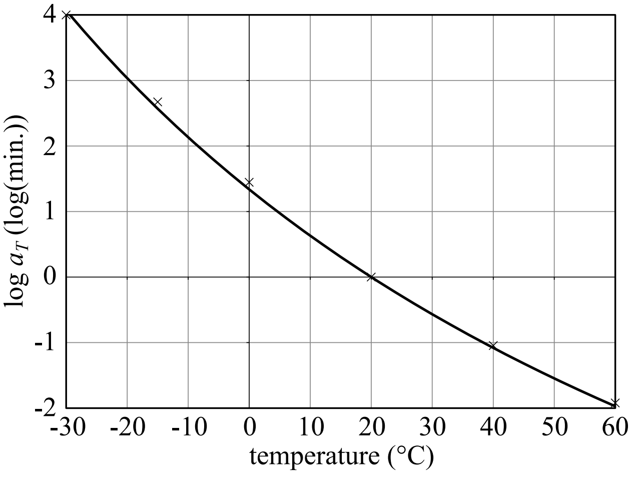

Fig. 4 Best fit curve (solid line) of the WLF equation to the measured shift parameter versus temperature data obtained for the unaged specimen (points).

III. Results and Discussion

The master curves were obtained for the aged specimens. The influence of aging time and aging at two different temperatures on the master curves is discussed in the following sections.

A. Effect of Aging at 60 °C on the Master Curve

Using the aforementioned method, four specimens were prepared by aging for 1, 2, 4, and 8 weeks at 60 °C in addition to the unaged specimen. These correspond to specimens E, F, G, H, and I, respectively, in Table 1. The measured master curves for each specimen are shown in Fig. 5, which plots the scaled relaxation modulus (multiplied by the factor T_{ref}/T) versus reduced time (time divided by a_T.) It can be seen that time-shifting the stress relaxation curves results in a continuous master curve. Thus, the assumption of the aged material being thermorheologically simple is valid at least over the temperature range tested. Other mechanisms may complicate the response at sufficiently low temperatures (below -30 °C) [16–18].

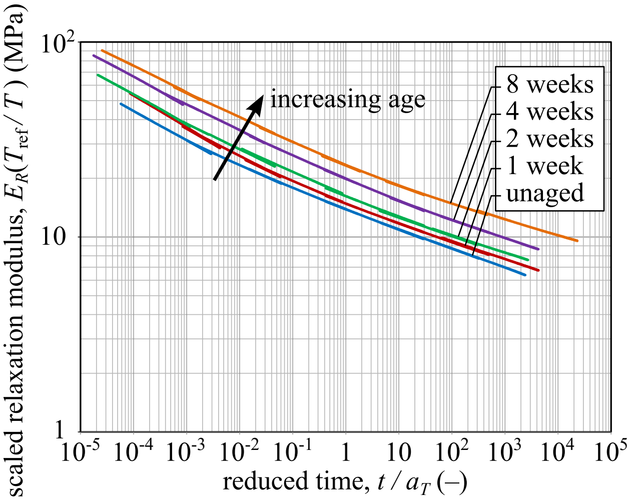

Fig. 5 Master curves for specimens aged at 60 °C for different lengths of time.

The general trend shows that aging shifts the master curve upwards due to an increase in the relaxation modulus. A longer heat treatment resulted in a larger shift in the master curve; the unaged and the 1, 2, 4, and 8 week aged specimens exhibited sequentially higher shifted master curves. Aging in HTPB propellant is mainly due to cross-linking, thus the longer aging times result in greater cross-linking. Cross-linking causes the propellant to have a higher modulus, which is consistent with an upward shift in the master curve. Considering the reduced time $t/a_T = 1$, the corresponding relaxation moduli for the unaged specimen and the aged specimens for 1, 2, 4, and 8 weeks were 13.8, 14.6, 16.2, 19.5, and 23.0 MPa, respectively.

B. Effect of Aging at 50 °C on the Master Curve

A second series of specimens were aged for 1, 2, 4, and 8 weeks at 50 °C, corresponding to specimens A, B, C, and D, respectively, in Table 1, and their master curves measured (shown in Fig. 6 along with the unaged specimen, I.) Unlike the results in Fig. 5 for 60 °C, trends in the master curves for differently-aged specimens at 50 °C are not as distinguishable. As can be seen in Fig. 6, the master curve for the specimen aged for one week is nearly the same as the unaged specimen. The master curves of specimens aged for 2, 4, and 8 weeks are clustered together at a higher relaxation modulus compared to the master curves of the unaged specimen and the specimen aged for one week. With the unaged specimen being the same as in Fig. 5, the relaxation moduli for the specimens aged at 50 °C for 1, 2, 4, and 8 weeks at time $t/a_T = 1$ are, respectively, 13.3, 18.3, 17.0, and 17.5 MPa.

This distribution of the master curves may be due to variability in the artificial aging process (e.g. humidity fluctuations.) In addition, fluctuations in the oven temperature were approximately ±5 °C during the aging of this series of specimens, which would affect the amount of cross-linking occurring in the specimen and the resulting relaxation modulus. For the specimens aged at 60 °C, the temperature fluctuations were smaller at approximately ±3 °C.

Comparing the master curves obtained via aging at 50 and 60 °C for 8 weeks shows that a higher aging temperature

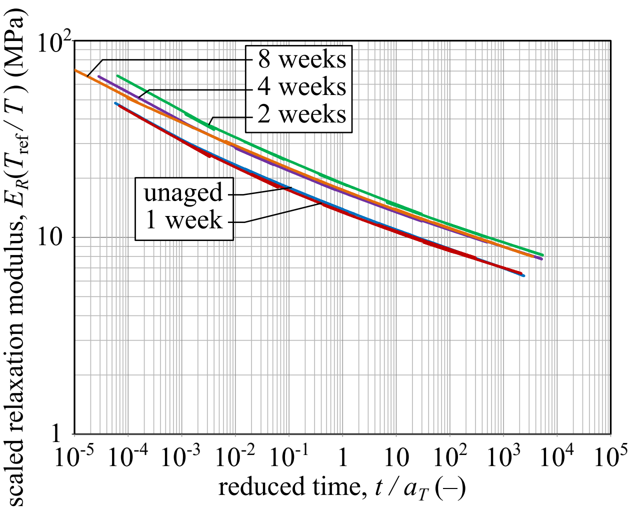

Fig. 6 Master curves for specimens aged at 50 °C for different lengths of time.

results in a higher relaxation modulus. This is consistent with the idea that cross-linking occurs at a higher rate at higher temperatures. In particular, the relaxation moduli of the specimens aged for 8 weeks at 50 and 60 °C at a reduced time of $t/a_T = 1$ are 17.5 MPa and 23.0 MPa, respectively.

C. Variability in the Master Curve of Aged Propellant

The variance of the master curve obtained from different specimens was determined by testing three specimens aged for the same length of time (8 weeks at 60 °C). The specimens were aged in a single oven at the same time and thus were approximately subjected to the same temperature history. The standard deviation was calculated using the method of pooled variances [19] with data from the three master curves at reduced times of 10^{-4}, 1, and 10^4. The standard deviation of the master curves was determined to be 8.41 MPa. This standard deviation of the master curves is higher than the standard deviation of previous relaxation tests at different temperatures of unaged specimens [15]. However, in the previous study, a higher standard deviation was observed for tests at lower temperatures when the specimen is stiffer than at high temperatures. This is consistent with a higher standard deviation measured for the aged specimens, which also become stiffer due to cross linking. The higher variance with the stiffer materials may be due to increased sensitivity to clamping effects. Although from a previous study [15], the DCB fixture in DMAs exhibited a smaller standard deviation than traditional uniaxial tension stress relaxation tests. In addition, the aging process may proceed differently between specimens due to variations in their initial properties. Future experiments will incorporate a more precise temperature control during artificial aging to reduce specimen variability.

IV. Conclusion

The master curves of aged HTPB-based propellant specimens were measured using a dynamic mechanical analyzer. Specimens were aged for different lengths of time and at two different temperatures. The ability to generate the master curves of the aged specimens confirmed that the typical time-temperature superposition approach (here using the WLF equation) is valid as the assumption of thermorheologically-simple material behavior holds.

Comparing the master curves of differently-aged specimens showed that specimens that were aged longer and at higher temperature tended to result in an upward shift in the master curve (higher relaxation modulus) relative to lesser-aged specimens. Comparing the unaged specimen to the specimen aged the most (8 weeks at 60 °C) showed that the relaxation modulus increased by approximately 67 %. The specimens aged at a higher temperature also exhibited a higher relaxation modulus with a 32 % increase observed in the specimen aged for 8 weeks at 60 °C compared to 50 °C. The increased relaxation modulus for aged specimens is consistent with the cross-linking process taking place, which tends to increase the modulus of the material. In summary, the modulus of HTPB-based propellant is estimated to increase by as much as 67 % over a natural aging period of 6 years. Ongoing experiments are testing multiple specimens under each aging condition to determine their average response. However, based on the experimental results in Fig. 5

and Fig. 6, it could be the case that 50 °C is not sufficiently high to cause significant aging after 8 weeks for specimens tested; hence the variation in master curves in Fig. 6 is dominated by specimen variation and aging effects are negligible. Meanwhile, a temperature of 60 °C is beginning to be sufficiently high to increase the significance of aging, which would result in the distinguishable trend between master curves for differently-aged specimens as shown in Fig. 5. To determine the relative significance of specimen variation versus aging, additional experiments should be performed for longer aged specimens at additional temperatures. Indeed, the appropriate aging temperature for a given specimen is an open question. Several previous studies have proposed different aging temperatures. For example, a previous study of aging of HTPB propellant suggested that artificial aging at 50 °C is sufficient for mimicking natural aging while aging at 60 °C initiates aging mechanisms that do not occur at room temperature during natural aging [20]. Nonetheless, the method described here for obtaining the master curve of aged propellant specimens will aid in answering these questions as it is more cost and time efficient compared to current approaches. In addition, master curves measured using this approach can be obtained in an efficient manner for use in finite element models (see [21] for example), which will improve the accuracy of lifetime predictions of solid rocket motors.

Acknowledgments

This work has been funded by the Air Force Research Laboratories Rocket Lab. The authors would like to thank AFRL for its full support. Dr. Wojnar's fellowship was funded by the AFOSR through the AFRL Summer Faculty Fellowship Program. In addition, the work performed here could not have been accomplished without the aid of fellow researchers in the NATO community.

References

[1] Chang, L.-S., "Investigation of Space Launch Vehicle Catastrophic Failures," *J Spacecr Rockets*, Vol. 33, No. 2, 1996, pp. 198 – 205.

[2] Ruderman, G., "Health Management Issues and Strategies for Air Force Missles," techreport ADA440133, Air Force Research Laboratory, Edwards Air Force Base, 2005.

[3] Hyde, R. S., "A Solid Rocket Motor Manufacturer's View of Sensors and Aging Surveillance," techreport ADA406078, ATK Thiokol Propulsion Corporation, Brigham City, UT, 2002.

[4] Ozupek, S., Tekkaya, E. A., Farris, R. J., and Liechti, K., "Computational Procedure for the Life Assessment of Solid Rocket Motors," *J Spacecr Rockets*, Vol. 47, No. 4, 2010, pp. 639 – 648.

[5] Yildirim, H. C., and Ozupek, S., "Structural Assessment of a Solid Propellant Rocket Motor: Effects of Aging and Damage," *Aerosp Sci Technol*, Vol. 15, No. 8, 2011, pp. 635 – 641.

[6] Williams, W. F., Landel, R. F., and Ferry, J. D., "The Temperature Dependence of Relaxation Mechanisms in Amorphous Polymers and Other Glass-Forming Liquids," *J Am Chem Soc*, Vol. 77, No. 14, 1955, pp. 3701 – 3707.

[7] Christensen, R. M., *Theory of Viscoelasticity*, Dover, Mineola, NY, 2003.

[8] Christiansen, A. G., Layton, L. H., and Carpenter, R. L., "HTBP Propellant Aging," *J Spacecr Rockets*, Vol. 18, No. 3, 1981, pp. 211 – 215.

[9] Ho, S. Y., "Viscoelastic Response of Solid Rocket Motor Components for Service Life Assessment," *J Mater Sci*, Vol. 32, No. 19, 1997, pp. 5155 – 5161.

[10] Wong, F. C., "Pseudodomain Fracture Analysis of Instrumented Analog Rocket Motors," *J Spacecr Rockets*, Vol. 40, No. 1, 2003, pp. 92 – 100.

[11] Keizers, H. J. L., "Accelerated aging of AP/HTPB Propellants and the Influence of Various Environmental Aging Conditions," techreport 124711, TNO Prins Maurits Laboratorium, Rijswijk, Netherlands, 1995.

[12] Cerri, S., Bohn, M. A., Menke, K., and Galfetti, L., "Ageing Behavior of HTPB Based Rocket Propellant Formulations," *Cent Eur J Energ Mater*, Vol. 6, No. 2, 2009, pp. 149 – 165.

[13] Bohn, M. A., "Prediction of Equivalent Time-Temperature Loads for Accelerated Ageing to Simulate Preset In-Storage Ageing and Time-Temperature Profile Loads," *40th International Annual Conference of ICT*, Karlsruhe, Germany, 2009.

[14] Cerri, S., Bohn, M. A., Menke, K., and Galfetti, L., “Aging of HTPB/Al/Ap Rocket Propellant Formulations Investigated by DMA Measurements,” *Propellants Explos Pyrotech*, Vol. 38, No. 2, 2013, pp. 190 – 198.

[15] Miller, T. C., Wojnar, C. S., and Louke, J. A., “Measuring Propellant Stress Relaxation Modulus Using a Dynamic Mechanical Analyzer,” *J Propul Power*, Vol. 33, 2017, pp. 1252 – 1259.

[16] De La Fuente, J. L., Fernandez-Garcia, M., and Cerrada, M. L., “Viscoelastic Behavior in a Hydroxyl-Terminated Polybutadiene Gum and its Highly Filled Composites: Effect of the Type of Filler on the Relaxation Processes,” *J Appl Polym Sci*, Vol. 88, No. 7, 2003, pp. 1705 – 1712.

[17] De La Fuente, J. L., and Rodriguez, O., “Dynamic Mechanical Study on the Thermal Aging of a Hydroxyl-Terminated Polybutadiene-Based Energetic Composite,” *J Appl Polym Sci*, Vol. 87, No. 14, 2003, pp. 2397 – 2405.

[18] Stacer, R. G., and Husband, D. M., “Small Deformation Viscoelastic Response of Gum and Highly Filled Elastomers,” *Rheol Acta*, Vol. 29, No. 2, 1990, pp. 152 – 162.

[19] Mandel, J., *The Statistical Analysis of Experimental Data*, Dover, New York, NY, 1984.

[20] Kivity, M., Hartman, G., and Achlama, A. M., “Aging of HTPB Propellant,” *41st AIAA/ASME/SAE/ASEE Joint Propulsion Conference & Exhibit*, Tuscon, AZ, 2005.

[21] Xu, J., Han, L., Zheng, J., Chen, X., and Zhou, C., “Finite Element Implementation of a Thermo-Damage-Viscoelastic Constitutive Model for Hydroxyl-Terminated Polybutadiene Composite Propellant,” *Mech Time-Depend Mater*, Vol. 21, No. 4, 2017, pp. 577–595.